ELASTOPLASTIC PROPERTIES UNDER NANO-MICROINDENTATION OF PHOSPHATE GLASSES DOPED WITH RARE-EARTH IONS

Z. Barbos

Institute of Applied Physics, str. Academiei 5, Chisinau, MD-2028 Republic of Moldova
E-mail: danitaz@mail.ru

(Received February 8, 2019)

Abstract

The microstructure and mechanical (elastic and plastic) properties of phosphate glasses (PhGs) doped with rare-earth elements (REEs), namely, Pr, Nd, Sm, Eu, Gd, Dy, Ho, Er, and Yb, have been studied in this paper. The strength parameters of the PhGs and their dependence on the load value modification have been estimated by the depth-sensing indentation method. Three specific stages have been revealed in the deformation process, including nano-, submicro, and microdeformation. It has been assumed that the elastic and plastic properties of PhGs can be associated with the specificity of the internal structure of the glasses.

1. Introduction

Intensive research into the various types of glassy materials is being conducted due to their widespread application in many areas of modern engineering. However, despite the progress made in understanding the internal structure of glassy materials on the nanometer scale, the problem of the structure of long-range order on the nano/micro/macro scale remains very hypothetical. Laser phosphate glasses (PhGs) have been intensively studied over the past decade, since (together with silicate glasses) they comprise an important group of compounds used in quantum electronics as active media of lasers, optical amplifiers, photosensitive elements, sensors, etc. [1–3]. Phosphate glasses are superior to their silicate counterparts in terms of optical properties. Knowledge of mechanical and microstructural characteristics is essential for detailed understanding of phenomena that occur during the manufacturing and processing of PhGs and strongly affect their operating parameters. Particularly, a correlation between structure and mechanical properties is determinative both in the reliability optimization of PhGs related to their use in optomechanical devices and in the design of other vitreous materials. The microstructure and mechanical properties of PhGs doped with ions of the rare-earth elements ((REEs), Pr, Nd, Sm, Eu, Gd, Dy, Ho, Er, Yb) were earlier analyzed in [4, 5]. In this paper, it is shown that other characteristics, such as "plasticity index" and "resistance index," are used to assess the mechanical properties of the materials and their resistance to plastic deformation, in addition to the well-known parameters *E* and *H*.

2. Experimental

The purpose of this paper is to study the mechanical properties of bulk PhGs belonging to the $Li_2O{\cdot}BaO{\cdot}Al_2O_3{\cdot}La_2O_3{\cdot}P_2O5{\cdot}R_2O_3$ and $SiO_2{\cdot}P_2O_5{\cdot}R_2O_3$ systems doped with REEs. The studied samples of PhGs were prepared by an unconventional ‘wet’ method [6]. Supervision of

microstructure evolution during the synthesis, processing, and operation of these materials will improve the nano- and micromechanical properties of these vitreous structures.

The microstructure of the sample surface was studied by optical, light (LM), and atomic force microscopy (AFM) methods. Mechanical parameters were studied by depth-sensing nano- and microidentation using a Nanotester PMT3-NI-02 device. The hardness and Young modulus calculations were carried out using the Oliver–Pharr method [7]. All of them were carried out automatically using the dedicated software.

3. Results and Discussion

Analysis of the surface microstructure of the samples using the LM method confirmed the data of [5], according to which all samples had a smooth surface without any cracks, pores, or defects. This finding indicates a high quality of the fine structure of the materials under study. Small globule-shaped entities of different colors were only observed on the polished surface of the samples (according to preliminary estimations, D_{gl} ~ 200–300 nm).

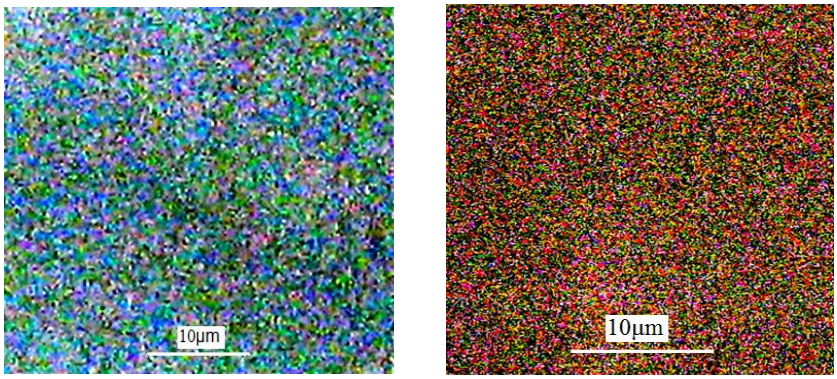

a b

Fig. 1. Surface morphology observed via LM for the PhGs samples doped with (a) Nd and (b) Pr.

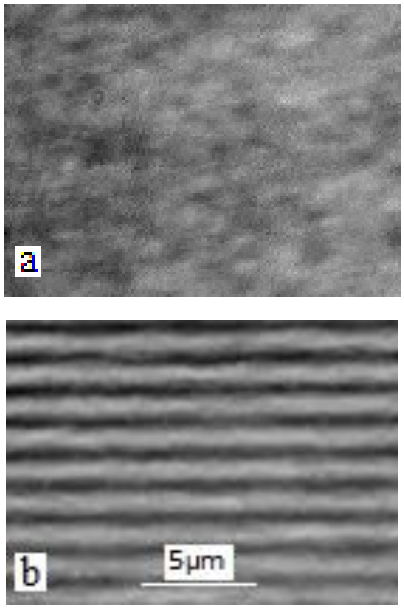

Fig. 2. LM images of the surface of the PhGs–Yb sample in (a) the normal and (b) interference mode.

This is confirmed by Fig. 1, which shows the regions of the surface of the PhGs doped with Nd and Pr. Figure 2 shows the surface relief in the interference regime for the sample containing an Yb impurity. A slight undulation of the interference lines caused by the presence of globules with a height of approximately 100 nm is observed on the surface.

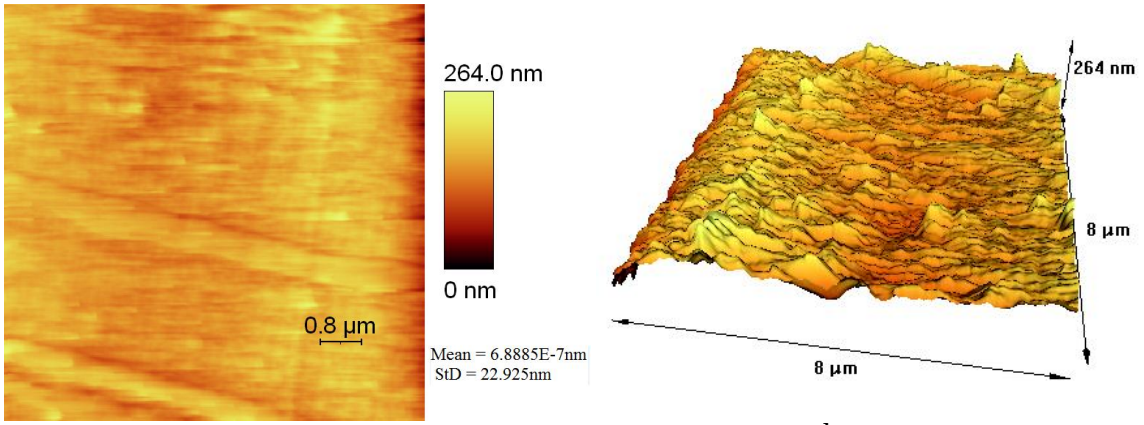

Fig. 3. (a) AFM data on the surface morphology of the sample doped with gadolinium (PhGs–Gd) and (b) a region of the surface of the PhGs–Gd sample recorded in the 3D mode.

Figure 3a shows the surface of the sample doped with gadolinium (PhGs–Gd). The pattern of globule distribution over the surface can be traced using this figure. It should be noted that the globules form unique tangles of different colors and dimension, since presumably they were formed from particles of various compositions. The same regularity can be seen for the other samples (Fig. 1). The undulated surface is more distinctly seen in the 3D mode of AFM (Fig. 3b).

Figure 4 shows results of the depth-sensing indentation tests. It should be noted that all the nano- and microindentation curves ($P(h)$) obtained for the samples under study were generally characterized by a smooth pattern of changes in the indentation depth at both the loading and unloading stages. In certain cases, at P_{max} = 500 and 900 mN, extremely slight inhomogeneity of the curves and weak undulation during the loading stage (PhGs–Yb, PhGs–Dy) were observed [5]. It is known from literature [8, 9] that breaking of atomic bonds leads to a decrease in the internal stresses in the indentation zone and thus causes an increase in the rate of penetration of the indenter into the material, due to which a nonuniform curve can be formed. Therefore, the shape of the obtained curves $P(h)$ provides data pertaining to the dynamics of the deformation process in the tested sample. Thereby, the smooth shape of the $P(h)$ curves in Fig. 4 indicates an uniform development of the process of the indenter deepening with increasing load, which can be the result of the sum of two processes, namely, the elastic compression of the crystal cell and the plastic deformation by the structure densification in the zone of load application [10, 11].

The Young's modulus (E) (Fig. 5a) and hardness (H) (Fig. 5b) exhibited a random dependence as a function of rare-earth ion atomic mass. Instead, it was found that the load value (P_{max}) affects H and E: a decrease in the peak load applied to the indenter (P_{max} = 900, 500, 100, 10 mN) was accompanied by an increase in the H and E values. The most

visible impact was observed in a range between 100 and 10 mN due to the indentation size effect (ISE) [12].

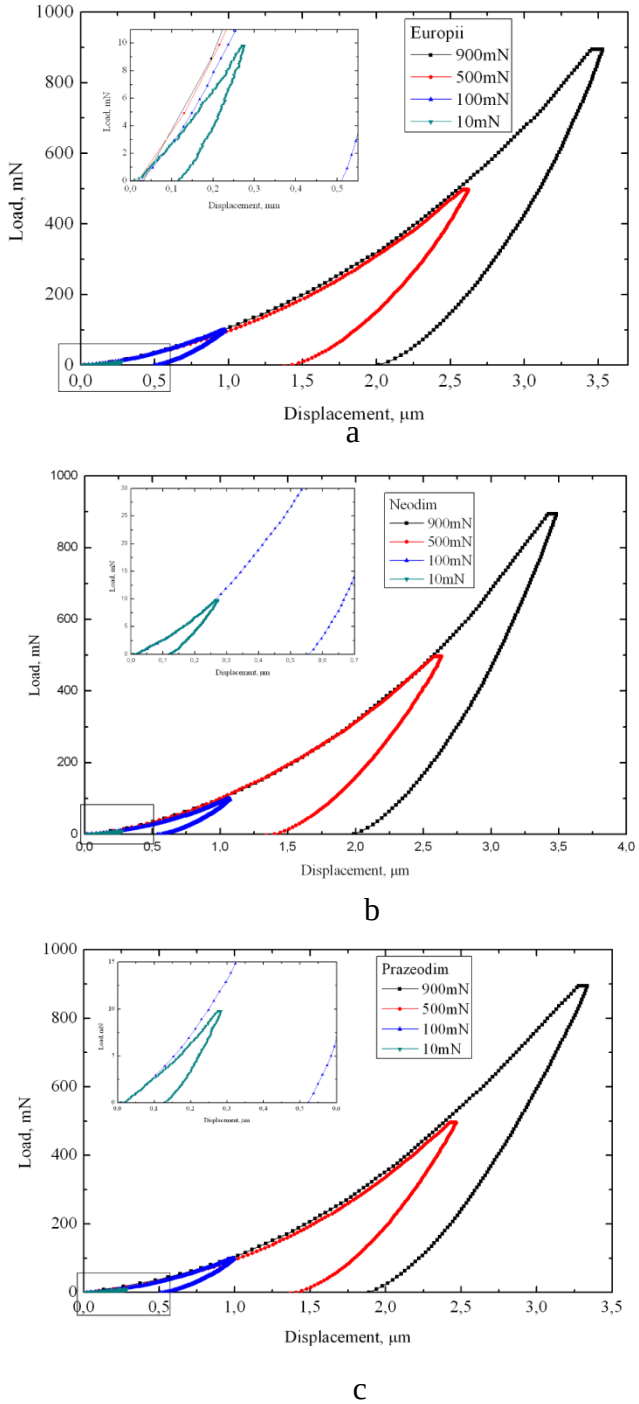

Fig. 4. Loading–unloading curves ($P(h)$) recorded at different maximum loads. Inserts: the curve for P_{max} = 10 mN on a larger scale; (a) PhG–Eu, (b) PhG–Nd, and (c) PhG–Pr.

The authors of [13] showed that the resistance of materials to plastic deformation can be determined using, in addition to well-known E and H parameters, other characteristics, such as "plasticity index" and "resistance index." These parameters describe the resistance of materials to deformation and destruction under an external concentrated load and are computed as the ratio of material hardness and Young's modulus, respectively, H/E and H^3/E^2 shown in Fig. 6. It is evident from Fig. 6 that both indexes, H/E and H^3/E^2, in common with the E and H dependences, mainly decrease with an increase in P_{max} for many studied materials. It means that the resistance to indenter penetration into the doped PhGs decreases with an increase in the load.

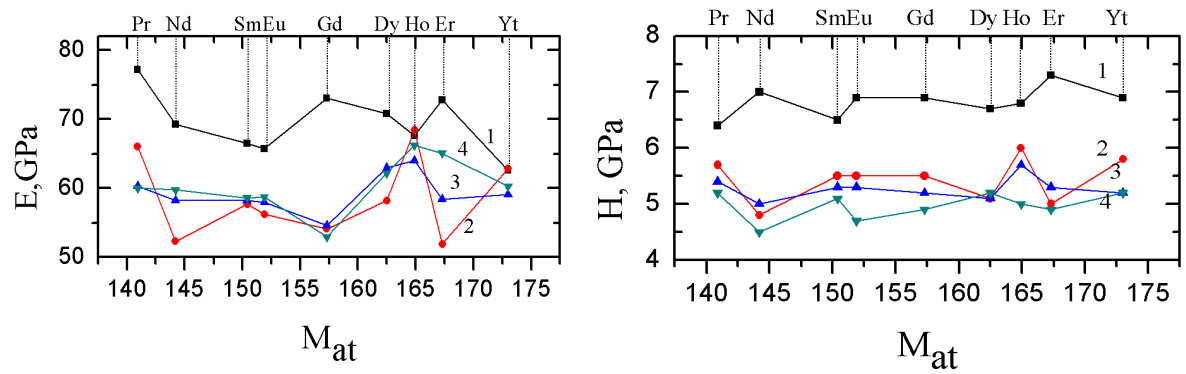

a b

Fig. 5. (a) Young modulus (E) and (b) hardness (H) as a function of REE atomic mass (M_{at}). The curves correspond to different peak values of applied load under depth-sensing indentation, P_{max} = (*1*) 10, (*2*) 100, (*3*) 500, and (*4*) 900 mN.

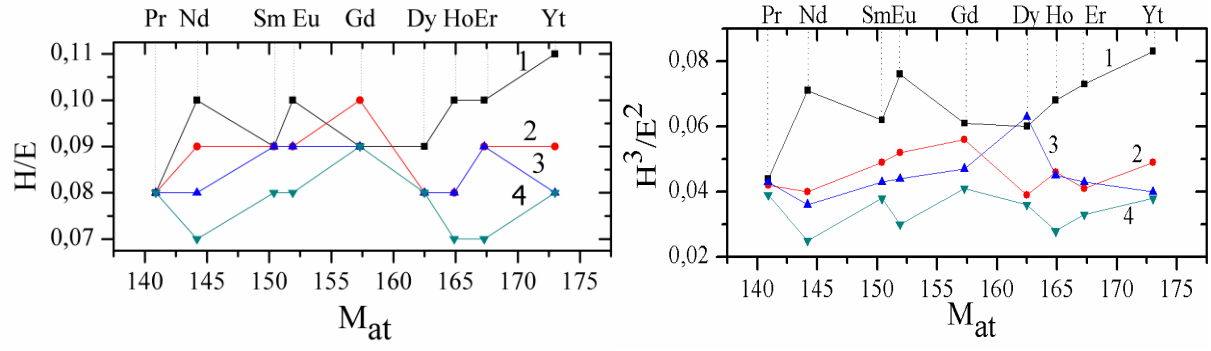

a b

Fig. 6. Variation in (a) plasticity index (H/E) and (b) resistance index (H^3/E^2) as a function of rare-earth ions atomic mass. The curves correspond to different peak values of applied load under depth-sensing indentation, P_{max} = (*1*) 10, (*2*) 100, (*3*) 500, and (*4*) 900 mN.

Comparison of the relationship between Young's modulus, hardness, plasticity indexm and resistance index with the size of ionic radii and the atomic mass of the doping REEs has not revealed a clear dependence between these parameters. Based on this fact, an assumption has been made that the elastic and plastic properties of PhGs–R are mainly determined by the internal structures of the glasses, which can contain rigid frameworks of icosahedral three-dimensional figures by analogy with the structure of the hardened gel revealed by the authors of [14].

4. Conclusions

The microstructure and mechanical properties of PhGs doped with REEs (PhGs–R, here R = Pr, Nd, Sm, Eu, Gd, Dy, Ho, Er, Yb) have been studied in this work. It has been shown that the fine structure of the surface consists of globules, which form unique tangles of different colors, presumably due to the fact that they are formed of particles with different compositions with diameters of ~200–300 nm and heights of <100 nm. The particles are appreciably densely—yet not uniformly—distributed over the surface and form a certain type of a framework structure.

The mechanical parameters, Young's modulus E, hardness H, plasticity index H/E, and resistance index H^3/E^2 exhibit a nonmonotonous dependence on the size of ionic radii and atomic mass of the doping REEs and on the load value under the depth-sensing indentation; in general, they exhibit a tendency toward decreasing with increasing load. An assumption has been made that the elastic and plastic properties of PhGs–R are mostly stipulated by the specificity of the internal structure of the glasses.

Acknowledgments

This work has been performed within the framework of the national project no. 15.817.02.06A.

References

[1] S. Jiang, T. Luo, B.C. Hwang, F. Smekatala, K. Seneschal, J. Lucas, and N. Peyghambarian, J. Non-Cryst. Solids 263–264, 364 (2000).
[2] W. Ruikun, J.D. Myers, and M.J. Myers, Proc. SPIE – Solid State Lasers X, 2001, vol. 4267, pp. 56–60.
[3] M.P. Bendett, N.A. Sanford, and D.L. Veasey, US Patent 490748, 2005.
[4] M. Elisa, C. Vasiliu, C. Grigorescu, B.A. Sava, A. Diaconu, H.J. Trodahl, and M. Dalley, Eur. J. Glass Sci. Technol. A 48 (5), 247 (2007).
[5] D.Z. Grabco, O.A. Shikimaka, M. Elisa, B.A. Sava, L. Boroica, C. Pyrtsak, A. Prisacaru, Z. Danitsa, I. Feraru, and D. Ursu, Surf. Eng. Appl. Electrochem. 48 (4), 365 (2012).
[6] M. Elisa, C. Vasiliu, C. Grigorescu, et al., Glass Tech.: Eur. J. Glass Sci. Technol. A 48 (5), 247 (2007).
[7] W.C. Oliver and G.M. Pharr, J. Mater. Res. 7 (6), 1564 (1992).
[8] Yu.S. Boyarskaya, D.Z. Grabco, and M.S. Kats, Fizika protsessov mikroindentirovaniya, Kishinev: Shtiintsa, 1986.
[9] Yu.S. Boyarskaya, R.P. Zhitaru, D.Z. Grabco, and V.A. Rahvalov, J. Mater. Sci. 33, 281 (1998).
[10] S. Yoshida, H. Sawasato, T. Sugawara, Y. Miura, and J. Matsuoka, J. Mater. Res. 25 (11), 2203 (2010).
[11] C. Hermansen, J. Matsuoka, S. Yoshida, H. Yamazaki, Y. Kato, and Y.Z. Yue, J. Non-Cryst. Solids 364, 40 (2013).
[12] W.D. Nix and H. Gao, J. Mech. Phys. Sol. 46 (3), 411 (1998).
[13] A. Leyland and A. Matthews, Wear 246 (1–2), 1 (2000).
[14] C.P. Royall, S.R. Williams, T. Ohtsuka, and H. Tanaka, Nat. Mater. 7, 556 (2008).